Structural Controllability Assessment for Inverter-Based Microgrids

Sandip Roy
Washington State University
Pacific Nortwest National Laboratory
Pulman, WA, USA
sandip@wsu.edu

Sinan G. Aksoy
Pacific Northwest National Laboratory
Seattle, WA, USA
sinan.aksoy@pnnl.gov

Subir Sarker
Washington State University
Pulman, WA, USA
subir.sarker@wsu.edu

Peng Wang
Pacific Northwest National Laboratory
Richland, WA, USA
peng.weng@pnnl.gov

Stephen J. Young
Pacific Northwest National Laboratory
Richland, WA, USA
stephen.young@pnnl.gov

***Abstract*—Enhanced inverter-based controls are considered for microgrids, which use additional actuation beyond a droop-like term. Shaping of the microgrid's small-signal dynamics using such enhanced controls is posed as a structural controllability problem. A graph-theoretic characterization of structural controllability is obtained, in terms of the concept of zero-forcing sets. Two benchmark test systems are used to illustrate the selection of locations where enhanced controls should be applied, based on the graph-theoretic analysis. These examples indicate that small-signal characteristics can be shaped using a relatively small number of enhanced controls.**

***Index Terms*—microgrid control, zero-forcing, structural controllability**

I. Introduction

Today's power distribution networkss are distinguished by the growing penetration of inverter-based distributed energy resources (DERs). These distribution-side energy generation and storage resources can provide additional margins and reduce losses during nominal operations where they are synchronized with the bulk grid, while also allowing portions of the grid (known as microgrids) to seamlessly switch to an isolated or islanded mode for off-nominal conditions. However, efficient and reliable operation of microgrids in both the grid-following and the islanded mode crucially depends on the regulation of each inverter's interface with the distribution network. With this motivation, there has been an energetic research effort on the regulation or control mechanisms used in interfacing inverters with the power distribution network [1], [2].

For microgrids operating in islanded mode, inverter controls are primarily designed with two concurrent goals in mind: 1) appropriate steady-state power sharing among the different DERs and 2) synchronization of microgrid frequency dynamics in the presence of small- and large- disturbances. With these goals in mind, several schemes have been proposed for regulating the electrical signal on the grid side of the inverter [3]–[8]. Among these schemes, droop controls have come to prominence for several reasons. First, they are entirely decentralized (i.e. do not require communications among the DERs in the microgrid). Further, because they mimic the controls used for mechanical power output regulation of inertial generators in the bulk grid, they can be seen to achieve desirable real and reactive power sharing and a frequency-synchronous operating point. In addition, measurement filtering and input-integration mechanisms used in the droop controls simulate the inertial physics of conventional generators, which guarantees small-signal stability of the synchronous operating point under broad conditions.

While droop controls have proved viable for microgrids, they also suffer from a number of drawbacks. First, inertia (or delay) can introduce poorly-damped system-wide oscillations, for certain load and generation patterns. Additionally, the performance of the droop controls with respect to dynamic responses across the range of possible operating points is challenging to evaluate. Thus, the tuning of droop controls may leave the system susceptible to instability or poor damping, which are hidden to the system designer. These potential drawbacks are of particular concern in the microgrid setting, because of the wide variability of operating points, the lack of redundancy in the network's topology, the presence of lines that are substantially resistive (not only reactive), the comparative decentralization of operations/planning as compared to the bulk grid, and the high susceptibility of the network to cyber and kinetic attacks. As a whole, more flexible and adaptive inverter controls may be needed to assure high performance and resilient microgrid operations.

Importantly, as a strong contrast with the bulk grid, inertial dynamics and droop controls are not dictated by physical laws

Sinan G. Aksoy, Peng Wang, and Stephen J. Young were supported by the Resilience through Data-driven Intelligently-Designed Control (RD2C) Initiative, under the Laboratory Directed Research and Development (LDRD) Program at Pacific Northwest National Laboratory (PNNL). PNNL is a multi-program national laboratory operated for the U.S. Department of Energy (DOE) by Battelle Memorial Institute under Contract No. DE-AC05-76RL01830. Sandip Roy conducted this research during an appointment at the U.S. National Science Foundation, supported by an Intergovermental Personnel Act agreement with Washington State University.

2021 North American Power Symposium (NAPS) | 978-1-6654-2081-5/21/$31.00 ©2021 IEEE | DOI: 10.1109/NAPS52732.2021.9654687

and hardware constraints in a microgrid: there is comparatively far greater flexibility to design the electrical signal on the grid side of the inverter. This flexibility potentially could be exploited to achieve desirable small-transient and large-transient response characteristics for typical load/generation patterns, and to adapt the controller to changing operating points and topologies. Additionally, microgrids are becoming increasingly data rich, with new sensing capabilities, algorithms for inferring network characteristics, and infrastructure for communicating remote data, which could also be used to improve and adapt inverter controls. Some studies have proposed alternative control strategies which seek to exploit these flexibilities [9].

In this study, we also consider the flexibility available in designing inverter controllers, but take a broader perspective focused on understanding the capacity for and limits on control. Precisely, our formulation models each inverter as not only using a nominal droop-like controller which achieves power sharing, but also having available an additional actuation or feedback of arbitrary form which can be used to further shape the small-signal respons. Based on this formulation, we seek to characterize these additional control channels from a structural perspective (i.e. across the range of possible network operating points), with the aim of understanding their capacity for shaping the small-signal dynamics. Here, we focus particularly on assessing controllability, as well as metrics for the required control energy, for these control channels. The analysis anticipates whether the control flexibility afforded by the inverter interface can allow for arbitrary shaping of the small-signal dynamics over the range of system operating points. Thus, the analysis shows the theoretical capacity for control of the microgrid small-signal dynamics through design or adaptation, provided appropriate information flow is made available to the inverter. In this sense, the analysis gives a bound on system resilience (ability to withstand and recover from disturbances over the range of operating solutions).

Our analyses build on a recent literature on structural controllability for canonical dynamical network models. For the microgrid model, we are able to develop a graph-theoretic characterization of structural controllability which parallels the existing results: specifically, a correspondence is shown between structural controllability and a notion known as zero-forcing of the network graph. This equivalence is appealing because it provides a starting point for developing computationally-friendly algorithms for assessing structural controllability and hence resilience. The equivalence also gives theoretical insight into topological determinants of controllability.

II. Problem Formulation

We are concerned with designing controllers to shape the small signal characteristics of an islanded microgrid with inverter-based DERs. A number of recent studies have analyzed the transient and small-signal dynamics of islanded microgrids with inverter-based DERs [3]–[8]. These various studies enforce desirable power sharing through the droop-like controls, and then assess the transient and small-signal responses through analysis of closed-loop nonlinear and linearized dynamical models. In contrast, in this study, we recognize the flexibility available in inverter control design by representing each inverter as having a droop-like control along with an additional designable input signal. For this enhanced model, we characterize the controllability of the system as a means to understand whether the available design flexibility can be exploited to achieve desirable small signal characteristics.

The transient and small-signal dynamics of the inverter-based microgrids have been carefully modeled in past work [3]–[6] so we give a summary presentation here, expanding only on the aspects that are new. In accordance with much of the literature, we assume a decoupling between the voltage angle dynamics and the voltage magnitude dynamics, and concentrate on characterizing the angle dynamics. This decoupling assumption is known to be apt provided that resistances in the network are relatively small, which is typically the case. In this case, the angle dynamics are known to be primarily dependent on the real power flow at network nodes, and hence only the real power characteristics and their control need be considered.

Formally, a connected microgrid with n buses, labeled $1,\ldots,n$, is considered. The admittance of the line between two buses i and k is denoted by $Y_{ik}\angle\phi_{ik} = G_{ik}+jB_{ik}$, where $G_{ik} \leq 0$ and $B_{ik} \geq 0$ are the conductance and susceptance of the line, respectively. These are all zero if there is no line between the buses i and k. A real power balance equation is satisfied at each bus i [6], [7]:

$$\begin{aligned} P_{G_i} &= P_{L_i}+\sum_{k=1}^{n} V_i V_k Y_{ik}\,\cos(\theta_i-\theta_k-\phi_{ik}) \\ &= P_{L_i}+V_i^2 G_{ii}+\sum_{k} V_i V_k Y_{ik}\,\cos(\theta_i-\theta_k-\phi_{ik}) \end{aligned} \quad (1)$$

where P_{G_i} and P_{L_i} are the generated active power and consumed (load) power at bus i, V_i is the magnitude of the voltage at bus i (assumed constant per the assumed decoupling), and θ_i is the angle of the voltage at bus i.

The load power at each bus can be modeled as a linear function of the bus frequency $\omega_i = (\dot{\theta}_i)$ (see [6]), as follows:

$$P_{L_i}=P^0_{L_i}+D_{L_i}\dot{\theta}_i \quad (2)$$

where, $P^0_{L_i}$ and $D_{L_i}\geq 0$ are the nominal load and the frequency coefficient of the load at bus i, respectively.

It remains to specify the real power generation P_{G_i} at each bus i in terms of the bus voltage. For buses without DERs, the real power generation is zero ($P_{G_i} = 0$). For buses with inverter-based DERs, the inverter control can be used to impose a dynamic relationship between the real power generation and the bus voltage angle. Specifically, with appropriate control mechanisms, the inverter can be made to approximate a voltage source, wherein the voltage magnitude and angle are selected by the control system. It is natural to use a control mechanism which sets the voltage angle in terms of measurements of the local real power (and potentially other network-wide measurements of real power or angles), which maintains the decoupling of the model and allows shaping of the steady-state real power and angle dynamics. Commonly, a control law is used which replicates the inertial dynamics of the bulk grid, as well as the droop control used to achieve a desirable power-sharing solution. This droop-like controller sets the inverter's electrical frequency (derivative of the angle) as a linear function of a measured local real power generation, which is a low-pass filtration of the actual power generation, with offsets selected to achieve a desirable power-sharing solution. Formally, for an inverter at bus i, the following Laplace-domain relationship is used:

$$s\theta_i = \frac{P_{G_i}^0 - P_{G_i}}{D_{R_i}} \times \frac{1}{1+T_{D_i}s} + \omega_0 \tag{3}$$

where, ω_0 is the system-wide reference angular frequency; $P_{G_i}^0$ is reference power which is the generated active power at the nominal frequency; $D_{R_i} \geq 0$ indicates the slope or gain of the frequency droop relationship of the inverter; T_{D_i} is the time constant for a first-order low-pass filter which is used to smooth variations and reduce noise in the measured power; and s is the Laplace variable. In this study, we modify the droop equation to assert that the droop feedback can be adjusted by an arbitrary input signal, which also could be set through a feedback mechanism, at a subset of the buses. With the modification, the droop equation in the Laplace domain for these buses becomes:

$$s\theta_i = \left(\frac{P_{G_i}^0 - P_{G_i} + u_i}{D_{R_i}} \right) \times \frac{1}{1+T_{D_i}s} + \omega_0, \tag{4}$$

where u_i is a designable input signal which modifies the frequency (angle derivative) at the bus. We note that we have also applied the low-pass filter to the input, to capture that this signal will typically use filtered measurements of local real power as well as other microgrid signals. The ensuing analysis can be easily modified to encompass the case that the the input is not filtered, or is filtered in a different way. However, we use this formulation because it captures the typical setting and also allows for a clearer analysis. The relationship can be expressed in the time domain as:

$$P_{G_i} = P_{G_i}^0 + u_i - D_{R_i}\dot{\theta}_i - D_{R_i}T_{D_i}\ddot{\theta}_i. \tag{5}$$

Equations (1)-(5) comprise a system of differential-algebraic equations which together specify the transient response of the microgrid. This system of equations can be linearized around an operating solution, and the algebraic equations either solved out or approximated with a singular perturbation argument, to obtain a state-space linear differential equation model for the small-disturbance response. Here, we have applied this procedure to obtain a linear differential equation model for the small-disturbance response. In doing so, we have used a singular perturbation approximation for the algebraic equations, which has the benefit of preserving the topological structure of the microgrid in the state-space model. Since this small-signal analysis has been detailed in prior work [6], here we simply present the form of linear differential equation model and omit the derivation and detailed expressions of the constituent matrices. The small-signal model takes the form:

$$\boldsymbol{\Delta\dot{x}} = \begin{bmatrix} 0_{n\times n} & I_{n\times n} \\ -L & -D \end{bmatrix} \boldsymbol{\Delta x} + \begin{bmatrix} 0_{n\times n} \\ B \end{bmatrix} \boldsymbol{u}, \tag{6}$$

where $\Delta\boldsymbol{x}$ is a vector containing the voltage angles and voltage frequencies (voltage angle derivates) at all buses, L is the Laplacian matrix associated with a directed graph (digraph) $\Gamma = (V, E)$, D is a nonnegative diagonal matrix, B is a matrix whose columns are indicator vectors of the inverter buses where inputs can be imposed, and $\mathbf{u}$ contains the designable input signals. The digraph Γ has n vertices corresponding to the n buses in the microgrid, with bidirectional edges between two vertices if and only if there is a line between the buses in the microgrid. Importantly, the edge weights in Γ are dependent on the operating point of the network, and hence are subject to variation. In consequence, the Laplacian matrix L is structural, in the sense that its off-diagonal entries may take on arbitrary or at least varying values.

In this initial study, our goal is to assess the controllability of the microgrid dynamic model from a graph-theoretic perspective. The challenge in the controllability analysis lies in the fact that the model is structural, i.e. the state matrix entries are subject to variation. Thus, we seek for conceptual and algorithmic results on controllability of the small-signal model. These results are meant to give insight into whether the flexibility afforded by microgrid controls, as captured in the availability of an assignable input, can be used to shape the small-signal responses over the range of operating points. In addition, we seek to find small sets of buses in the microgrid such that inputs at those locations are sufficient for controllability, and hence can be leveraged to shape the small-signal response. In addition assessing the controllability, we also study control energy metrics in the context of an example, to gain insight into the practicality of these controls.

III. Results

Our main aim in this section is to develop a graph-theoretic characterization of controllability for the microgrid small-signal model (Equation 6), and to use this characterization to identify sets of buses in the network model that can be used to shape the small-signal dynamics. As noted above, we are interested in understanding whether control is possible and developing control schemes given a particular graph structure, but over a range of model parameter values. Thus, we focus on a structural controllability analysis of the microgrid model. In fact, we find it convenient to undertake the analysis for a broader class of models, as described next.

Formally, given a class of matrices $\mathcal{M}$ in $\mathbb{R}^{n\times n}$ and diagonal matrices $\mathcal{D} \in \mathbb{R}^{n\times n}$, we are interested in identifying the sets S (which we call leader sets) such that

$$\boldsymbol{\ddot{x}} = M\boldsymbol{x} + D\boldsymbol{\dot{x}} + \left(\sum_{s\in S} e_s e_s^T \right) \boldsymbol{u} \tag{7}$$

is controllable for any choice of $D \in \mathcal{D}$ and $M \in \mathcal{M}$. We will denote the collection of such subsets by $\mathcal{S}(\mathcal{D}, \mathcal{M})$. In this study, we seek to determine the collection of such sets $\mathcal{S}(\mathcal{D}, \mathcal{M})$ for the microgrid model, and discuss implications for microgrid control.

We undertake this analysis in several steps. First, the controllability of the system model is equivalenced with the controllability of a first-order system (Section III.A). Then, the equivalence is used together with previous results to develop a graph-theoretic condition for controllability for the microgrid model (Equation 6), see Section III.B; specifically, controllability is characterized in terms of a graph-theoretic construct known as a zero-forcing set [10]–[12]. This graph-theoretic relationship is then used to determine the collection of leader sets allowing for control in several example microgrid networks (Section III.B). Implications of these characterizations are discussed, and the energy required for control is also explored for one of these examples. As a whole, the analyses indicate that there is substantial flexibility to shape the microgrid small-signal model, including to smooth oscillations, by applying advanced controls at a small set of network locations.

A. Formal Results: Controllability Equivalence

In this initial study, we focus on the uniform damping case (that is, the case where $\mathcal{D} = \{\mu \boldsymbol{I}_{n\times n} \colon \mu \in \mathbb{R}\}$). This is a common assumption for small-signal models of both the bulk power grid and microgrids, and often reasonably captures small-signal behaviors in the model. For this special case, the controllability of the second order system on n variables (Equation 7) can be reduced to the controllability of a first-order system on n variables. This reduction allows application of previously-developed graph-theoretic results on controllability, motivating the following equivalence.

Theorem 1. *The system $\dot{\boldsymbol{x}} = A\boldsymbol{x} + B\boldsymbol{u}$ is controllable if and only if the system $\ddot{\boldsymbol{x}} = A\boldsymbol{x} + \mu\dot{\boldsymbol{x}} + B\boldsymbol{u}$ is controllable.*

Proof. Before proceeding it is helpful to explicitly transform the second-order system to the following first-order (state-space) system:

$$\begin{bmatrix}\dot{\boldsymbol{x}}\\ \ddot{\boldsymbol{x}}\end{bmatrix} = \begin{bmatrix}0_{n\times n} & I_{n\times n}\\ A & \mu I_{n\times n}\end{bmatrix}\begin{bmatrix}\boldsymbol{x}\\ \dot{\boldsymbol{x}}\end{bmatrix} + \begin{bmatrix}0_{n\times n}\\ B\end{bmatrix}\mathbf{u}.$$

Now, recall that a first-order system is controllable if and only if the dimension of the left-nullspace of the Kalman contollability matrix is zero, i.e. the controllability matrix has full row-rank. To this end let $\mathcal{C}_1$ be the Kalman controllability matrix of the first-order system and let $\mathcal{C}_2$ be the Kalman controllability matrix of the second-order system. We will show that the dimension of the left-nullspace of $\mathcal{C}_2$ is the square oftwicethe dimension of the left-nullspace of $\mathcal{C}_1$. In particular, for $z_1, z_2 \in \mathbb{R}^n$ such that (z_1, z_2) is in the left-nullspace of $\mathcal{C}_2$, we will show that z_1, z_2 are both in the left-nullspace of $\mathcal{C}_1$.

We note first that the contollability matrix $\mathcal{C}_2$ consists of $2n$ blocks, with each block having the form

$$\begin{bmatrix}0_{n\times n} & I_{n\times n}\\ A & \mu I_{n\times n}\end{bmatrix}^k \begin{bmatrix}0_{n\times n}\\ B\end{bmatrix}$$

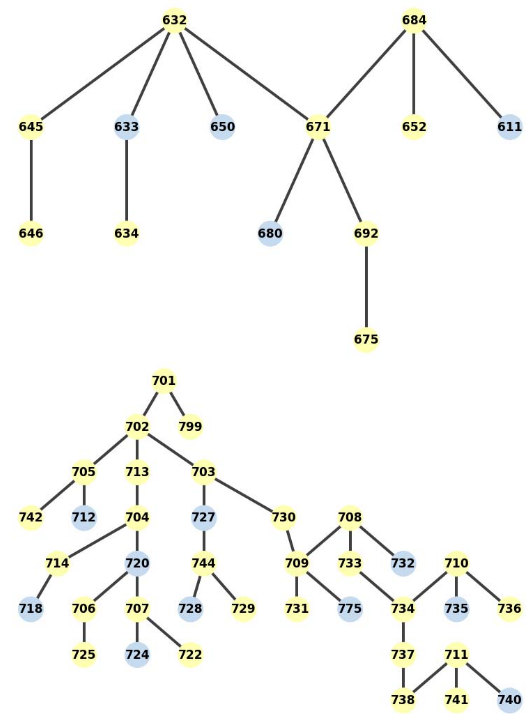

Fig. 1. Examples of minimal zero-forcing sets (in blue) for the 13-bus (top) and 37-bus (bottom) benchmark systems.

for k in the range $0, \ldots, 2n-1$. Inductively expanding the powers of the state matrix, the k^{th} block can be rewritten as

$$\begin{bmatrix}\sum_{j=0}^{\lfloor k-1/2\rfloor}\binom{k-1-j}{j}\mu^{k-1-2j}A^jB\\ \sum_{j=0}^{\lfloor k/2\rfloor}\binom{k-j}{j}\mu^{k-2j}A^jB\end{bmatrix}.$$

Now suppose that $z_1, z_2 \in \mathbb{R}^n$ such that (z_1, z_2) is in left-nullspace of $\mathcal{C}_2$. Considering the first two blocks of $\mathcal{C}_2$, we have that

$$\begin{bmatrix}z_1\\ z_2\end{bmatrix}^T\begin{bmatrix}0\\ B\end{bmatrix} = 0 + z_2^TB = 0$$

and

$$\begin{bmatrix}z_1\\ z_2\end{bmatrix}^T\begin{bmatrix}B\\ \mu B\end{bmatrix} = z_1^TB + \mu z_2^TB = z_1^TB = 0.$$

Thus $z_1^TB = z_2^TB = 0$. Now supposing that $z_1^TA^iB = z_2^TA^iB = 0$ for $i = 0, \ldots, \ell-1$ consider the $(2\ell)^{\text{th}}$ and $(2\ell+1)^{\text{th}}$ blocks in the controllability matrix $\mathcal{C}_2$. For these two blocks we have

$$\begin{bmatrix}z_1\\ z_2\end{bmatrix}^T\begin{bmatrix}\sum_{j=0}^{\ell-1}\binom{2\ell-1-j}{j}\mu^{2\ell-1-2j}A^jB\\ \sum_{j=0}^{\ell}\binom{2\ell-j}{j}\mu^{2\ell-2j}A^jB\end{bmatrix} = z_2^TA^\ell B$$

and

$$\begin{bmatrix}z_1\\ z_2\end{bmatrix}^T\begin{bmatrix}\sum_{j=0}^{\ell}\binom{2\ell-j}{j}\mu^{2\ell-2j}A^jB\\ \sum_{j=0}^{\ell}\binom{2\ell+1-j}{j}\mu^{2\ell+1-2j}A^jB\end{bmatrix} = \begin{matrix}z_1^TA^\ell B \quad +\\ (\ell+1)\mu z_2^TA^\ell B\end{matrix}.$$

As a consequence, $z_1^TA^\ell B = z_2^TA^\ell B = 0$. Thus, by induction, $z_1^TA^\ell B = z_2^TA^\ell B$ for $\ell = 0, \ldots, n-1$ and z_1, z_2 are in the left-nullspace of $\mathcal{C}_1$. The relationship between the dimensions of the left-nullspaces of $\mathcal{C}_1$ and $\mathcal{C}_2$ follows immediately and $\mathcal{C}_1$ is full row-rank if and only if $\mathcal{C}_2$ is full row-rank. $\square$

It is worth mentioning that the primary obstruction to extending Theorem 1 to arbitrary diagonal matrices D is the non-commutativity of the multiplication between A and D.

B. Formal Results: Graph-Theoretic Characterization

In what follows we will restrict our attention to the uniform damping case. In our development, as a slight abuse of notation, we use $\mathcal{S}(\mathcal{M})$ to represent $\mathcal{S}(\mathcal{D}, \mathcal{M})$ when $\mathcal{D}$ is restricted to multiples of the identity.

Our aim here is to first give a graph-based characterization of controllability for the microgrid small-signal model. Recall specifically that we are interested in the controllability of

$$\ddot{\boldsymbol{x}} = -L\boldsymbol{x} + D\dot{\boldsymbol{x}} + B\boldsymbol{u},$$

where $L = L(\Gamma)$ is restricted by the structure of the microgrid as defined by the digraph Γ. The values taken by L are encompassed by the structural sets defined in [10], as follows. For a fixed digraph $\Gamma = (V, E)$, we define

$$\mathcal{Q}(\Gamma) = \left\{ X \in \mathbb{R}^{n\times n} \colon \text{for } i \neq j, X_{ij} \neq 0 \Leftrightarrow (i,j) \in E(\Gamma) \right\}$$
and
$$\mathcal{L}(\Gamma) = \{ X \in \mathcal{Q}(\Gamma) \colon X\mathbb{1} = 0 \}.$$

Our interest is in determining structural controllability of the microgrid small-signal model for a given leader set, and hence determining the collection of leader sets that achieve controllability, i.e. $\mathcal{S}(\mathcal{L}(\Gamma))$. As $\mathcal{L}(\Gamma) \subseteq \mathcal{Q}(\Gamma)$, we have that $\mathcal{S}(\mathcal{L}(\Gamma)) \subseteq \mathcal{S}(\mathcal{Q}(\Gamma))$. Furthermore, by Theorem 1, controllability of the second-order model reduces to that of a first-order model. Therefore, from the work of Monshizadeh et al. [10], controllability can be reduced to a graph-theoretic test on Γ, and the collection of controllability-achieving leader sets $\mathcal{S}(\mathcal{Q}(\Gamma))$ can be described precisely in terms of the combinatorial structure of Γ. Specifically, these sets are exactly related to the notion of *zero-forcing sets* for the graph Γ, which we define next.

The zero-forcing sets of a graph are defined by a vertex-coloring process. In particular, a subset $S \subseteq V(\Gamma)$ is called a *zero-forcing set* if coloring all $u \in S$ blue and all $u \notin S$ white, and repeatedly then applying the following coloring rule:

- *Coloring Rule:* If u is blue and has exactly one neighbor w which is white, then change the color of w to white.

will eventually change the color of all vertices in Γ to blue. Figure 1 contains an example of a *minimal* zero-forcing set of a graph. Using the language of zero-forcing, we have the following main result:

Theorem 2. *The dynamical system*

$$\ddot{\boldsymbol{x}} = -L\boldsymbol{x} + \mu\dot{\boldsymbol{x}} + \left(\sum_{s\in S} e_s e_s^T\right)\boldsymbol{u}$$

where L *is the Laplacian matrix for a digraph* Γ *is controllable if* S *is a zero-forcing set of* Γ.

It is worth noting that for some graphs Γ, the inclusion $\mathcal{S}(\mathcal{L}(\Gamma)) \subseteq \mathcal{S}(\mathcal{Q}(\Gamma))$ is strict, i.e. the class of microgrid small-signal models is narrower than the generic structural set defined by [10]. Thus, there may be additional controllability-achieving leader sets S which are not captured by Theorem 2. For example, as noted in [10], when Γ is the star $K_{1,3}$, the central vertex by itself belongs to $\mathcal{S}(\mathcal{L}(K_{1,3}))$ but it is not a zero-forcing set. While there has been some work focusing on identifying the elements of $\mathcal{S}(\mathcal{L}(\Gamma)) - \mathcal{S}(\mathcal{Q}(\Gamma))$ for various graphs Γ, see for instance [13], [14], the deep connections between zero-forcing and linear algebra [15] means that, in practice, it is typically easier to identify an element of $\mathcal{S}(\mathcal{Q}(\Gamma))$. For example, while identifying the size of a minimal zero-forcing set for a graph G is $\mathcal{NP}$-complete in general [16], even when searching for certain restricted solutions, such as connected zero-forcing sets [17]. In the case that Γ is an undirected tree, zero-forcing sets can be efficiently constructed using the connection with path covers [15], [18]. Of particular relevance the determination of zero-forcing sets for graphs associated with the power grid (and microgrids) is the work of Row [19], which provides upper and lower bounds on the size of a minimal zero-forcing set based on the zero-forcing of the components after removing a cut-vertex from the graph.

C. Examples

We apply and discuss these concepts on two well-known test systems, published by the IEEE Distribution System Analysis Subcommittee Report[1]:

- 13-bus Feeder: a small example of a distribution network with unbalanced loading conditions.
- 37-Bus Feeder: located in California, this feeder has a 4.8 kV operating voltage.

For each test system's graph, we conduct an exhaustive search to find all minimal zero-forcing sets. In the case of the 13-bus system, there are 28 possible minimal zero forcing sets of size 4, whereas the 37-bus system has 4800 minimal zero forcing sets of size 10. In general, finding all possible minimal zero-forcing sets is prohibitively expensive, since finding a minimal zero-forcing set is $\mathcal{NP}$-hard. Nonetheless, it is straightforward to check whether a given set is zero-forcing; Figure 1 illustrates examples of a particular minimal zero-forcing set for each system, which (via the aforementioned coloring rule) can be easily seen to be zero-forcing sets.

From the perspective of microgrid control, the zero-forcing sets indicate sets of network buses where enhanced inverter-based controllers can be applied to shape the small-signal dynamics of the microgrid at will. In particular, our results show that the inverter voltage angles at the buses corresponding to a zero-forcing set can be designed to move the state of the dynamical model to any desired value regardless of the operating point of the system, since the system is controllable. More importantly, from standard control-theory machinery [20], controllability also implies that feedback controllers can be designed for this set of nodes to place the closed-loop

[1]https://site.ieee.org/pes-testfeeders/resources/

eigenvalues of the system at will, which means that oscillations can be damped and time-constants shortened.

We have undertaken a simulation of the small-signal dynamics of the 13-bus feeder to illustrate the potential benefit of the enhanced inverter controls proposed here and the associated graph-theoretic analysis. For the simulation, all 13 buses were assumed to have inverter-connected DERs which are amenable to control. Loading patterns for the network were assumed to vary in such a way that steady-state phase angle differences across each line would vary between 0^o and 60^o. Nominally, droop-like controllers were applied at each bus. The small-signal dynamics of the model, as described above, was simulation. The droop-controlled model is seen to have multiple pairs of oscillatory modes, with a minimum damping ratio of about 7% for a heavily-loaded scenario. The zero-forcing analysis of the 13 feeder network described above has identified sets of four buses, where controllers can be applied to place the closed-loop eigenvalues at will and hence eliminate or damp these oscillations. Thus, the graph-theoretic analysis allows for selection of relatively sparse sets of network locations where enhanced controllers can be applied to improve on the performance achieved by droop-like controllers.

To test the practicality of control from such controllability-achieving leader sets, we have also characterized the controllability Gramian of the system at inputs at these locations, for a couple of different zero-forcing sets: the example shown in Figure 1 (Case A), as well as an alternative where an input is applied at Bus 680 rather than Bus 675 (Case B). For each case, we have found statistics of the trace of the inverse of the controllability Gramian over 100 simulations, which is an integrative measure of required control effort, over 100 stochastically-selected operating points. For Case A, the inverse Gramian trace was found to have a mean of 1320, with a maximum value of $1.85E4$. For Case B, the inverse Gramian trace was found to have a mean of 537, with a maximum value of 7330; thus, we see that Case B allows for shaping of the microgrid small-signal dynamics with comparatively less effort. We stress that the maximum trace values for both cases are orders of magnitude smaller than for other input locations that are not zero-forcing sets. The control energy analysis gives some empirical evidence that zero-forcing sets give practical selections for network locations where advanced controls should be applied.

IV. Conclusions

We have explored how the flexibility inherent to inverter-based controls can be exploited to shape the small-signal dynamics of islanded microgrids. Our analysis suggests that this flexibility can be used to substantially improve the small-signal dynamics of the microgrid, as compared to a standard droop control. The formulation presented here provides a means to leverage standard controls-engineering techniques such as pole placement to shape the small-signal responses of microgrids.

References

[1] M. A. Hossain, H. R. Pota, W. Issa, and M. J. Hossain, "Overview of ac microgrid controls with inverter-interfaced generations," *Energies*, vol. 10, no. 9, p. 1300, 2017.

[2] I.-Y. Chung, W. Liu, D. A. Cartes, E. G. Collins, and S.-I. Moon, "Control methods of inverter-interfaced distributed generators in a microgrid system," *IEEE Transactions on Industry Applications*, vol. 46, no. 3, pp. 1078–1088, 2010.

[3] N. Pogaku, M. Prodanovic, and T. C. Green, "Modeling, analysis and testing of autonomous operation of an inverter-based microgrid," *IEEE Transactions on power electronics*, vol. 22, no. 2, pp. 613–625, 2007.

[4] J. Schiffer, R. Ortega, A. Astolfi, J. Raisch, and T. Sezi, "Conditions for stability of droop-controlled inverter-based microgrids," *Automatica*, vol. 50, no. 10, pp. 2457–2469, 2014.

[5] Y. Song, D. J. Hill, and T. Liu, "Small-disturbance angle stability analysis of microgrids: A graph theory viewpoint," in *2015 IEEE Conference on Control Applications (CCA)*. IEEE, 2015, pp. 201–206.

[6] A. Al Maruf, M. Ostadijafari, A. Dubey, and S. Roy, "Small-signal stability analysis for droop-controlled inverter-based microgrids with losses and filtering," in *Proceedings of the Tenth ACM International Conference on Future Energy Systems*, ser. e-Energy '19. New York, NY, USA: Association for Computing Machinery, 2019, p. 355–366. [Online]. Available: https://doi.org/10.1145/3307772.3328310

[7] N. Ainsworth and S. Grijalva, "A structure-preserving model and sufficient condition for frequency synchronization of lossless droop inverter-based ac networks," *IEEE Transactions on Power Systems*, vol. 28, no. 4, pp. 4310–4319, 2013.

[8] W. Du, Z. Chen, K. P. Schneider, R. H. Lasseter, S. Pushpak Nandanoori, F. K. Tuffner, and S. Kundu, "A comparative study of two widely used grid-forming droop controls on microgrid small-signal stability," *IEEE Journal of Emerging and Selected Topics in Power Electronics*, vol. 8, no. 2, pp. 963–975, 2020.

[9] B. B. Johnson, M. Sinha, N. G. Ainsworth, F. Dörfler, and S. V. Dhople, "Synthesizing virtual oscillators to control islanded inverters," *IEEE Transactions on Power Electronics*, vol. 31, no. 8, pp. 6002–6015, 2015.

[10] N. Monshizadeh, S. Zhang, and M. K. Camlibel, "Zero forcing sets and controllability of dynamical systems defined on graphs," *IEEE Transactions on Automatic Control*, vol. 59, no. 9, pp. 2562–2567, 2014.

[11] M. Doostmohammadian and U. A. Khan, "Minimal sufficient conditions for structural observability/controllability of composite networks via kronecker product," *IEEE Transactions on Signal and Information processing over Networks*, vol. 6, pp. 78–87, 2019.

[12] L. A. Smith and I. V. Hicks, "Optimal sensor placement in power grids: Power domination, set covering, and the neighborhoods of zero forcing forts," *arXiv preprint arXiv:2006.03460*, 2020.

[13] H. Tanner, "On the controllability of nearest neighbor interconnections," in *2004 43rd IEEE Conference on Decision and Control (CDC) (IEEE Cat. No.04CH37601)*, vol. 3, 2004, pp. 2467–2472 Vol.3.

[14] A. Rahmani, M. Ji, M. Mesbahi, and M. Egerstedt, "Controllability of multi-agent systems from a graph-theoretic perspective," *SIAM Journal on Control and Optimization*, vol. 48, no. 1, pp. 162–186, 2009.

[15] AIM Minimum Rank – Special Graphs Work Group, "Zero forcing sets and the minimum rank of graphs," *Linear Algebra and its Applications*, vol. 428, no. 7, pp. 1628–1648, 2008. [Online]. Available: https://www.sciencedirect.com/science/article/pii/S0024379507004624

[16] A. Aazami, "Hardness results and approximation algorithms for some problems on graphs," Ph.D. dissertation, University of Waterloo, 2008.

[17] B. Brimkov and I. V. Hicks, "Complexity and computation of connected zero forcing," *Discrete Applied Mathematics*, vol. 229, pp. 31–45, 2017.

[18] P. J. Slater, "Path coverings of the vertices of a tree," *Discrete Mathematics*, vol. 25, no. 1, pp. 65–74, 1979. [Online]. Available: https://www.sciencedirect.com/science/article/pii/0012365X79901535

[19] D. D. Row, "A technique for computing the zero forcing number of a graph with a cut-vertex," *Linear Algebra and its Applications*, vol. 436, no. 12, pp. 4423–4432, 2012, special Issue on Matrices Described by Patterns. [Online]. Available: https://www.sciencedirect.com/science/article/pii/S0024379511004174

[20] W. J. Rugh, *Linear system theory*. Prentice-Hall, Inc., 1996.